Journal of
Alzheimer's Disease & Parkinsonism

Research Article   **Open Access**

Calpain-Mediated Hsp70.1 Cleavage in Monkey CA1 after Ischemia Induces Similar 'Lysosomal Vesiculosis' to Alzheimer Neurons

Tetsumori Yamashima[1*], Arumugam Mathivanan[1], Maryia Y. Dazortsava[1], Shota Sakai[2], Shota Kurimoto[1], Hong Zhu[1], Nozomi Funaki[1], Hanbai Liang[1], Françoise Hullin-Matsuda[2], Toshihide Kobayashi[2], Hiroyasu Akatsu[3], Hitoshi Takahashi[4] and Yoshio Minabe[1]

[1]Departments of Restorative Neurosurgery and Psychiatry, Kanazawa University Graduate School of Medical Science, Kanazawa, Japan
[2]Lipid Biology Laboratory, RIKEN (Institute of Physical and Chemical Research), Wako, Japan
[3]Choju Medical and Neuropathological Institute, Fukushimura Hospital, Aichi, Toyohashi, Japan
[4]Department of Pathology, Brain Research Institute, University of Niigata, Niigata, Japan

Abstract

For the past decade evidence has gathered for the implication of lysosomes in the development of programmed cell death. Recent data advocate for dual roles of heat-shock protein 70.1 (Hsp70.1) not only as a molecular chaperone for damaged/aged proteins but also as a guardian of lysosomal integrity. Hsp70.1-mediated lysosomal stabilization is tightly regulated, but its disorder under extreme conditions results in lysosomal rupture to cause cell death. Comparing with the pathological hallmark 'granulo-vacuolar degenerations' in Alzheimer's disease, the postischemic monkey neurons were carefully observed with microscope. Intriguingly, we found very similar change, and identified it as 'lysosomal vesiculosis' by electron microscopy. However, the exact molecular and structural impacts of the Hsp70.1 disorder upon the lysosomal membrane are hardly elucidated in the human brain because of the practical and ethical problems. Accordingly, using the monkey brain tissues after *in-vivo* and *in-vitro* oxidative stresses, we studied molecular modifications of Hsp70.1 and its counterpart bis(monoacylglycero) phosphate (BMP), because these molecules are closely related to the lysosomal membrane stability by regulating acid sphingomyelinase. It still remains unelucidated whether ischemia/reperfusion can alter composition or amount of BMP in the brain. Regardless of the brain regions studied, the normal monkey brain tissues showed calpain-mediated cleavage of Hsp70.1 after *in-vitro* oxidative stress. In the CA1 after *in-vivo* ischemia/reperfusion, we first found that docosahexaenoic and oleic acids in BMP showed a significant decrease on days 1 and 3, compared to non-ischemic controls. Since Hsp70.1-BMP binding is indispensable for activating acid sphingomyelinase and producing ceramide to stabilize lysosomal membrane, dysfunction of Hsp70.1 and BMP presumably causes storage of sphingomyelin and deficiency of ceramide at the lysosomal membrane, leading to its destabilization in the postischemic CA1 neurons. These data, combined together, suggest that lysosomal destabilization induced by calpain-mediated cleavage of carbonylated Hsp70.1 and the concomitant BMP breakdown causes 'lysosomal vesiculosis'.

Keywords: Neuronal death; Hsp70.1; BMP; Lysosome; Calpain-cathepsin hypothesis; Cerebral ischemia; Alzheimer's disease

Abbreviations: AD: Alzheimer's Disease; ALLN: N-Acetyl-Leu-Leu-Nle-CHO; ASM: Acid Sphingomyelinase; BMP: Bis(Monoacylglycero) Phosphate; CA1: Cornu *Ammonis* 1; DG: Dentate Gyrus; H-E: Hematoxylin-Eosin; Hsp70.1: Heat-Shock Protein 70.1; HNE: 4-Hydroxy-2-Nonenal; K-B: Kluver-Barrera; Lamp-2: Lysosome-Associated Membrane Protein-2; LFB: Luxol Fast Blue; ROS: Reactive Oxygen Species

Introduction

The potential danger of the accidental release of lysosomal hydrolases was initially recognized by de Duve, who discovered lysosome and called it a "suicide bag" [1]. However, the detailed mechanism of lysosomal rupture was unknown until the 'calpain-cathepsin hypothesis' was formulated using the monkey experimental paradigm by Yamashima et al. [2]. They claimed that μ-calpain and cathpsin B and L are main players during the propagation and execution phases of programmed neuronal necrosis after cerebral ischemia/reperfusion. Activated μ-calpain translocates to lysosomal membranes after ischemia to disrupt them, and the subsequent spillage of cathepsins into the cytoplasm and neuropil eventually dismantles the whole CA1 neurons [2,3]. Cell death induced by lysosomal rupture occurs essentially by a distinct mechanism from apoptosis in which the affected cells preserve their lysosomal membrane integrity until the last moment.

Nowadays, Alzheimer's disease (AD) is the most common form (~60%) of dementia in the aged population. In the brain affected by AD, neuronal death occurs mainly in the hippocampus, entorhinal cortex, frontal, parietal and temporal cortices [4]. Neurons in the hippocampal CA1 and layer II of the entorhinal cortex are particularly vulnerable. Amyloid β, the main constituent of senile plaques, exacerbates oxidative stress and causes peroxidation of cell membranes which ultimately leads to neuronal death [5,6]. Etiology of the vast majority of AD, i.e. late-onset sporadic cases, still remains unknown, but may include age-related increases in oxidative stress, impaired energy metabolism and perturbed cellular Ca^{2+} homeostasis due to age-related reduction of the cerebral blood flow. An imbalance between the rate of synthesis, aggregation and clearance of unwanted and misfolded proteins, causes accumulation of proteins such as toxic amyloid β and tau oligomers and subsequent neurodegeneration in AD [7].

Because of its high O_2 consumption and inadequate equippment with antioxidant defense systems, the brain is prone to oxidative stress [8]. Reactive oxygen species (ROS) play important physiological functions, including gene expression, signal transduction, and defense against invading pathogens. However, ROS can also cause extensive cellular damage by an imbalance between the ROS generation and the antioxidant defense capacity of the body. The exact molecular mechanism of ROS-mediated cellular damage is not entirely clear. It remains grossly unknown whether the presence of oxidatively-damaged molecules could simply reflect secondary epiphenomena or having a causal role [9]. ROS modify polyunsaturated fatty acids of the lipid membrane, and lipid peroxidation leads to the formation of highly reactive malondialdehyde and 4-hydroxy-2-nonenal (HNE) [10,11]. In particular, HNE is a strong electrophile and has the ability to readily adduct and damage proteins [12]. Increased carbonylation of heat-shock protein 70.1 (Hsp70.1; simply Hsp70, also called Hsp72) by the lipid peroxidation product HNE, was recently found to cause ischemic neuronal death in the monkey hippocampus [13-16].

It is recently accepted that vascular risk factors linked to cerebrovascular disease and stroke significantly increase the risk of developing AD. Since ischemic events in the elderly induce amyloid precursor protein, amyloid β and tau pathology, cerebral ischemia might be a key factor in the formation of the full picture of Alzheimer neurodegeneration over years [17-20]. Most AD cases show silent ischemic episodes that can cause neuronal death, blood-brain barrier changes, inflammation response, neurofibrillary tangles and amyloid plaque formation [20,21]. It is conceivable that Alzheimer neuronal death may be triggered by silent brain ischemia that activates calpain over years. Alzheimer neuronal death occurs by defective cholesterol trafficking within the endocytic/lysosomal pathway caused by activated calpain-mediated cleavage of oxidative stress-injured Hsp70.1 [16]. Hsp70.1 dysfunction due to its cleavage leads to deprivation of ceramide at the lysosomal membrane via decrease of BMP, and eventually to destabilization of lysosomal membranes.

Here, the mechanism of neuronal death was studied focusing its pathogenic relationship to the morphologic intracellular hallmark i.e. granulo-vacuolar degenerations. Molecular chaperone Hsp70.1-mediated autophagy is tightly regulated, but its disorder under extreme conditions results in neuronal death by the lysosomal destabilization. The aim of this study is to analyze influence of calpain activation and oxidative stress on the development of lysosomal vesiculosis, with particular attentions to Hsp70.1 and BMP. Since lysosomal vesiculosis was identified in neurons of both ischemic monkey and human Alzheimer neurons, it is suggested that a decreased lysosomal catabolism of membrane phospholipid might be a factor causing lysosomal destabilization.

Materials and Methods

Ischemia and sampling surgery

The monkey experiments were performed with the Guide for the Care and Use of Laboratory Animals as adopted and promulgated by National Institutes of Health (Bethesda, MD, USA). Furthermore, the experimental purposes and procedures were in accordance with the guidelines of Animal Care and Ethics Committee of Kanazawa University.

Japan monkeys (*Macaca fuscata*, weight 5-8 kg, total number=41) were used: for light microscopic analysis (n=3 for the control, days 3, 5, 7 and 9, respectively), electron microscopic analysis (n=1 for the control, days 1, 3, 5 and 7), Western blot analysis (n=1 for the control, days 3, 5, 7 and 9) and quantification of molecular species of BMP (n=4 for the control, days 1, 3 and 7).

Transient whole brain ischemia was induced by clamping both the innominate and left subclavian arteries for 20 min after resecting the sternum [3]. On days 1, 3, 5, 7 or 9 after the ischemia/reperfusion, the monkeys were anesthetized again and the brain was quickly removed for the Western blotting and molecular species analyses. Then, the tissue samples of hippocampal CA1 were resected with microscope, snap-frozen in liquid nitrogen, and stored at -85°C until analysis. Simultaneously, the non-ischemic tissue samples of CA1, dentate gyrus (DG), motor cortex, cerebellar cortex, substantia nigra, thalamus, putamen, globus pallidus, and medulla oblongata were resected for the *in-vitro* experiments.

Light and electron microscopy

Monkey experiments: After an anesthetic overdose, the monkeys were intracardially perfused with 0.5 L of saline followed by 2 L of 4% paraformaldehyde for the light microscopic analysis or by 2 L of 5% glutaraldehyde for the electron microscopic analysis. For the light microscopic analysis, after the brain was removed, tissue blocks were cryoprotected in 30% sucrose, frozen, and 40 μm thick coronal cryosections were sequentially cut.

For light microscopy, 5 μm sections of the paraffin-embedded tissues after fixation in 4% paraformaldehyde were stained with hematoxylin and eosin (H-E) and luxol fast blue (LFB). For electron microscopy, small specimens after glutaraldehyde perfusion were further fixed with 2.5% glutaraldehyde for 2h and subsequently with 1% osmium tetroxide for 1h at 4°C; the specimens were embedded in the epon-araldite mixture. The ultrathin sections were stained with uranyl acetate and lead citrate.

Alzheimer patients: This study was carried out in accordance with the Helsinki Declaration. The study protocol was approved by the ethical committee of Fukushimura Hospital and written informed consent was obtained from all subjects or their relatives. All AD and control patients were hospitalized to the Fukushimura Hospital, and autopsy was done with an informed consent within a few hours after death.

The brains from 5 patients with AD (male: female=2:3, age range=74-83 years, average=79.6 years) were studied. The AD patients showed moderate to severe dementia, which comprised of 74 year-old female, 88-year-old female showing old, healed subdural hematoma with cerebral contusion in the left hemisphere, 76-year-old-male, 83 year-old-female showing multiple lacunar infarctions, and 77-year-old male showing old small subcortical hematoma in the right parieto-occipital lobes. The accurate diagnosis of AD was done by several doctors regarding neuropathological staining. Age-matched non-AD 5 subjects (male: female= 4:1, age range=62–89 years, average=75.6 years) were studied as controls. They comprised of 78 year-old male showing multiple cerebral infarctions, 85 year-old male showing central pontine myelinolysis, 89 year-old female showing traumatic cerebral contusion in the frontal lobe, 62 year-old male showing old cerebral contusions in the perieto-temporal lobes, and 84 year-old male showing spinal epidural metastatic cancer.

The brain regions studied were hippocampus, basal ganglia, parietal cortex, frontal cortex, amygdala and cingulated gyrus. For the light microscopic analysis, thin sections of the paraffin-embedded tissues after fixation in 10% formaldehyde were stained with H-E, Bodian, and Kluver-Barrera (K-B) stainings as well as amyloid β and tau immunostainings.

Immunofluorescent analysis: Immunohistochemical analysis was done to examine the localization of Hsp70.1 in the normal and postischemic CA1 neurons. Thin (7 μm) sections were deparaffinized in xylene, rehydrated through graded ethanol, washed in PBS, and incubated with 0.1% trypsin for 30 min. Each primary antibodies were anti-human antibodies, comprising of monoclonal anti-human HSP70 (diluted 1:1000, Santa Cruz Biotechnology, Santa Cruz, USA), polyclonal anti-lysosome-associated membrane protein-2 (Lamp-2) (diluted 1:100, LifeSpan Biosciences, Seattle, USA), polyclonal anti-HNE antibody (diluted 1:1000, Alpha Diagnostic, San Antonio, TX, USA), monoclonal anti-HNE antibody (25 μg/ml, Japan Institute for the Control of Ageing, Shizuoka, Japan), monoclonal anti-BMP antibody 6C4 (diluted 1:50, Kobayashi et al., [22]); Echelon Biosciences, Salt lake city, UT, USA), and polyclonal (diluted 1:300, Kikuchi and Imajoh-Ohmi [23]) anti-activated μ-calpain antibody. Goat anti-rabbit IgG or anti-mouse IgG conjugated with Alexa Fluor 488 or 546 (Invitrogen, Eugene, Oregon, USA) were used as the secondary antibodies.

Slides were observed by a laser confocal microscope (LSM510, Carl Zeiss). Quantification of the fluorescent intensity was carried with LSM 510 META software.

Western blotting: To demonstrate activation of μ-calpain in the monkey hippocampal CA1 tissue after ischemia/reperfusion, we used two kinds of rabbit anti-activated μ-calpain which were made independently by Saido et al. [24] (1:300-1,000 dilution) (1992) or Kikuchi and Imajoh-Ohmi [23] (1:300 dilution) (1995). Both revelaed the same results.

To demonstrate calpain-mediated Hsp70.1 cleavage *in-vitro*, immunoblotting analysis was done to examine whether activated μ-calpain can *in vitro* cleave Hsp70.1 that was involved in the homogenated brain tissues of the non-ischemic monkey. Each homogenate was incubated at 0°C for 30 min after adding 0.5 U purified calpain (Calbiochem, La Jolla, CA, USA) plus 1.0 mM of CaCl$_2$ (Wako Pure Chemical, Osaka, Japan) mixed without or with 1.0 mM of H$_2$O$_2$ (Wako Pure Chemical, Osaka, Japan) and 500 μM of HNE (Calbiochem, La Jolla, CA, USA).

To examine whether the cleavage of carbonylated Hsp70.1 by activated μ-calpain is blocked by a specific μ-calpain inhibitor N-acetyl-Leu-Leu-Nle-CHO (ALLN), various concentrations (0,2,5,10,50,100 μM) of ALLN (Calbiochem, La Jolla, CA, USA) were added with 0.5 U activated μ-calpain to the normal CA1 homogenate samples that were incubated with 500 μM HNE for 60 min at 37°C.

The protein samples (20 μg) from the CA1 homogenates after incubation were separated by 15% SDS–PAGE gel and transferred on the PVDF membrane (ATTO, Tokyo, Japan). Primary antibody was purified mouse anti-human HSP70 that recognizes amino acid 429-640 residue (BD Biosciences, San Jose, CA, USA), while the secondary antibody was horseradish peroxidase conjugated anti-mouse IgG (Santa Cruz Biotechnology, Santa Cruz, USA).

Quantification of molecular species of BMP by LC-MS: Total lipids were extracted from the CA1 tissues of control and postischemic monkeys according to the method of Bligh and Dyer [25]. An Agilent 1100 series LC (Agilent Technologies, Santa Clara, CA) coupled to a 4000 QTRAP hybrid triple quadrupole mass spectrometer (AB SCIEX, Foster City, CA) was used to quantify the individual BMP. Extracted lipids (2 μl) were injected onto a reversed phase C18 column (CAPCELL PAK C18 MG III, 2.0×50 mm, Shiseido CO., LTD., Tokyo, Japan) and were eluted with an isocratic flow (100 μl/min) of methanol : acetonitrile=90 : 10 containing 5 mmol/L ammonium formate and 0.1% formic acid. The optimal

conditions for ionization and fragmentation of BMP were determined. MS analysis was run in the positive ion mode with following instrument parameters: curtain gas of 10, ion spray voltage of 5500, temperature of 250, nebulizer gas of 40, auxiliary gas of 50 and collision cell exit potential of 10. The levels of declustering potential, entrance potential and collision energy were optimized for each target. Multiple-reaction monitoring (MRM) mode was used to measure the BMP species, containing different acyl chains. Each ion pair of BMP species in MRM was monitored for 100 ms with a resolution of unit. BMP contents were calculated by relating the peak areas of each species to the peak area of the corresponding internal standard (C14:0/C14:0-BMP) and the standard curve of each internal standard (0-20 pmol). Data acquisition and analysis were performed using Analyst Software version 1.4.1 (AB SCIEX).

Statistics: The data of immunofluorescent analysis were mean ± SEM from n=3 monkeys for each group. Using GraphPads Prism 5 (Oberlin, San Deiego, CA, USA), statistical significance was determined by one-way ANOVA with Dunnett to compare the postischemic groups with the control. The data of molecular species of BMP were mean ± standard deviation from n=4 monkeys for each group. T-test analysis was done to compare means of two groups. $p<0.05$ was considered statistically significant.

Results

Light microscopy (granulo-vacuolar degenerations)

Humans: Granulo-vacuolar degenerations are characterized by the intraneuronal accumulation of large (up to 5 μm diameter) membrane-bound vacuoles harbouring a central granule. Because of the two-layer structure of limiting membranes at the electron microscopic level, it has been assumed to be autophagic organelles [26]. In this study, granulo-vacuolar degenerations were generally observed in all of the 5 Alzheimer brains regardless of the brain regions studied. Most of the neurons free from neuronal death showed central chromatolysis, and approximately half of the survivng neurons showed granulo-vacuolar degenerations (Figure 1). However, in the age-matched 5 control brains, only slight degree of granulo-vacuolar degenerations were observed by careful observation in one case, indicating that they are very exceptional in the non-AD elderly.

Monkeys: On day 3 after transient whole brain ischemia, the CA1 neurons showed shrinkage of the cell body and pyknosis of the nucleus. On day 5, the CA1 sector showed an almost complete loss of pyramidal neurons, showing a pallor apperance on the LFB staining (Figure
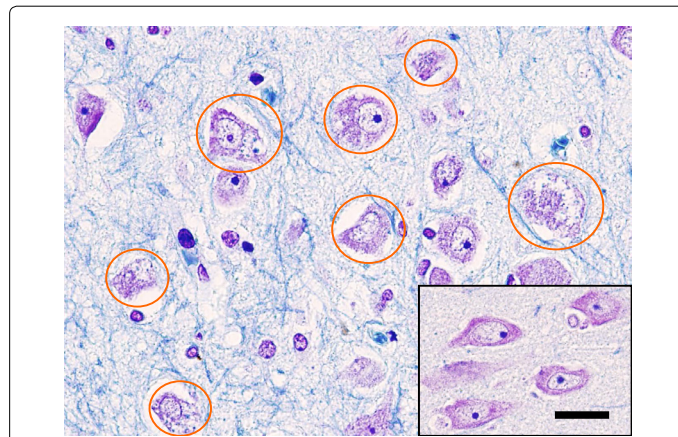

Figure 1: Granulo-vacuolar degenerations (red circles) are frequently seen in the Alzheimer neurons, but is scarecely seen in the age-matched control neurons (rectangle). CA1, K-B staining, Scale bar=20 μm.

2-A). On days 5~7, most of the degenerating CA1 neurons melted away, losing their configuration, and the cell debris was phagocytised by microglia. The remaining ghost neurons appeared as eosinophilic coagulation necrosis on H-E staining that was characterized by reddish cytoplasm with a complete loss of organella and diffusely-condensed nucleus containing a prominent nucleolus. At the high-magnified observation, microvacuolatory changes were seen in the degenerated perikarya (Figure 2-A arrow).

Electron microscopy (lysosomal vesiculosis): Since granulo-vacuolar degenerations were difficult to detect with light microscope in the postischemic monkey neurons, they were studied with electron microscope. Microvacuolatory changes in the postischemic CA1 neurons at the microscopic level (Figure 2-A) were ultrastructurally identified to be lysosomal vesiculosis; multivesicular bodies that appear within lysosomes on days 1~7 after ischemia/reperfusion (Figure 3).
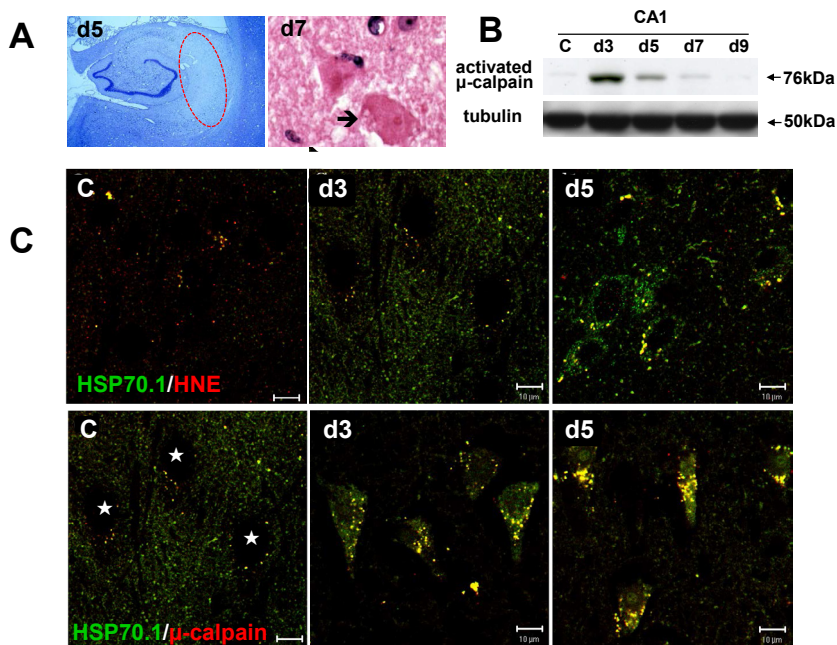

Figure 2: Dynamic change of expressions of Hsp70.1, HNE and activated μ-calpain, and CA1 neuronal death.
A: CA1 neuronal death is completed, showing a pallor appearance (dot red circle) on LFB staining on day 5 after ischemia/reperfusion. At the high magnification, CA1 neurons showing eosinophilic coagulation necrosis on H-E staining exhibit microvacuolatory changes on day 7 (arrows).
B: Western blotting shows a maximal activation of μ-calpain on day 3 after ischemia/reperfusion.
C: Hsp70.1, HNE and activated μ-calpain are upregulated altogether on days 3 and 5 after ischemia/reperfusion, being colocalized together.
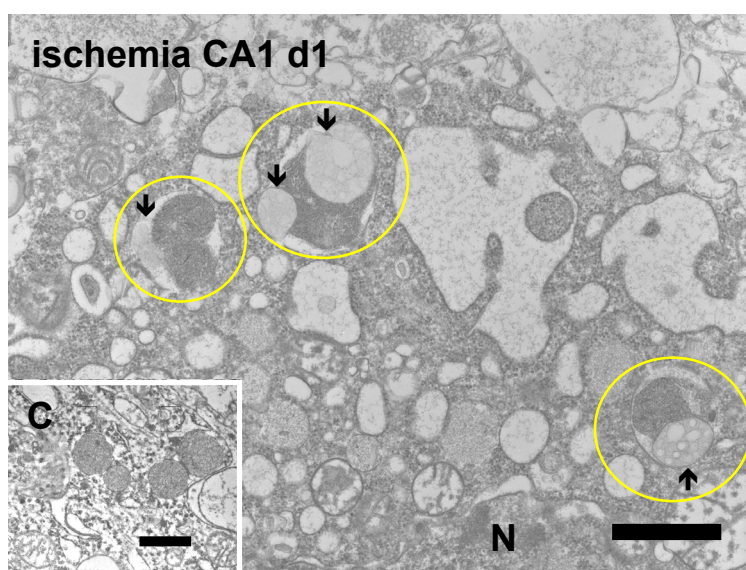
Figure 3: Electron microphotographs of the control (C) and postischemic day 1 (d1) monkey CA1 neurons. Compared to the normal lysosomes (open arrows, rectangle), the lysosomes on day 1 after ischemia/reperfusion reveal early features of lysosomal vesiculosis (yellow circles) that were characterized by accumulation of internal vesicles (arrows). N= nucleus, Scale bar=1 μm.

At the high-power electron microscopic observation, accumulation of internal vesicles being limited by two-layer membranes were found to occur adjacent to the lysosomal dense granules as early as on day 1 after ischemia/reperfusion. Such multivesicular lysosomes were never seen in the non-ischemic CA1 neurons (Figure 3, rectangle). They were ultrastructurally very similar to those observed in human Alzheimer neurons, but the size of each vesicle was less than 0.2 μm, being smaller compared to the Alzheimer neurons [16].

Western blotting

μ-calpain activation, *in-vivo*: Time-dependent change of the expression of activated μ-calpain was analyzed using two distinct polyclonal antibodies that can specifically recognize the 76-kDa activated form. The positive reaction using these antibodies indicates activation of μ-calpain in the given tissue. An increased expression of activated μ-calpain was seen after ischemia/reperfusion, compared to the control (Figure 2-B). Activation of μ-calpain was maximal on day 3. As a weak band was still seen on day 7 but not on day 9, μ-calpain activation in the monkey CA1 tissues was thought to be sustained as long as 7 days after ischemia/reperfusion.
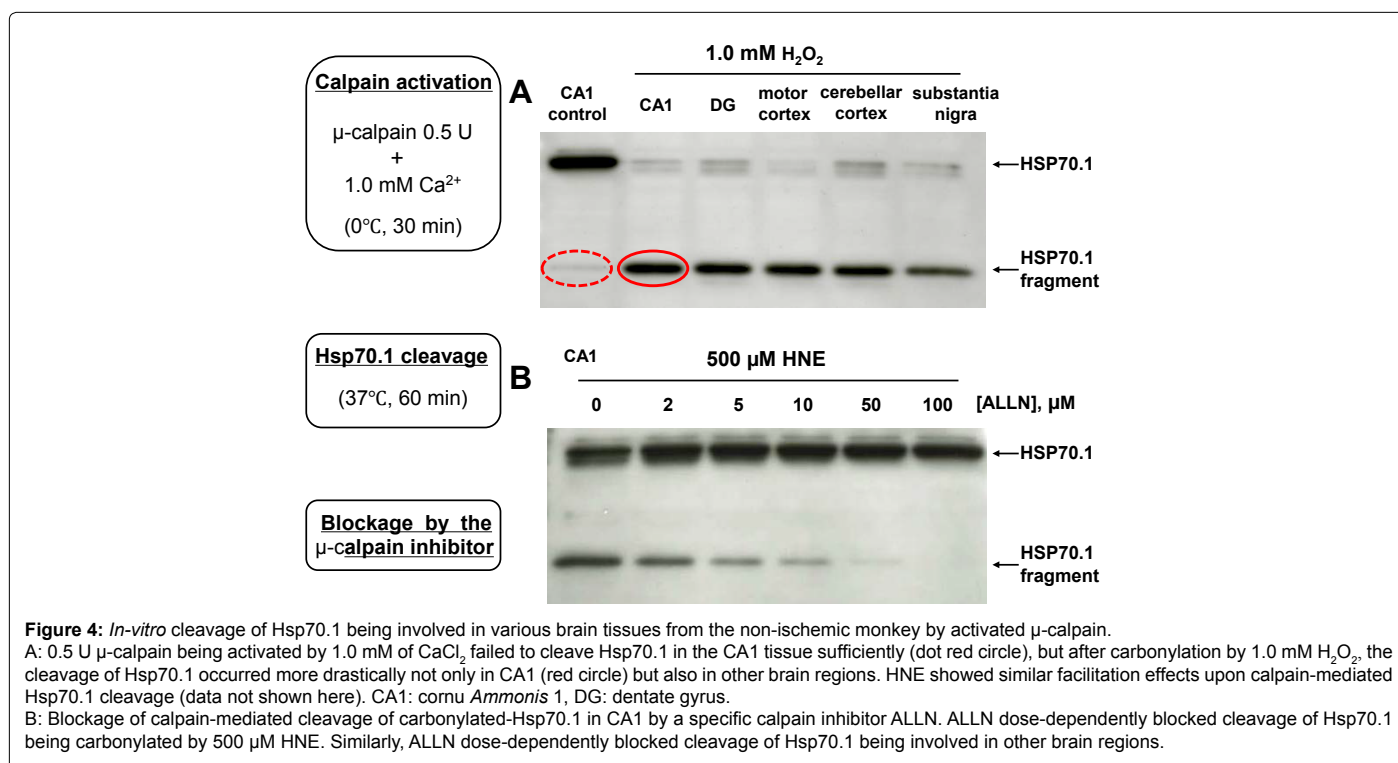
Calpain-mediated Hsp70.1 cleavage, *in-vitro*: After incubation of the homogenated non-ischemic tissues of CA1, DG, motor cortex, cerebellar cortex and substantia nigra in 1.0 mM $CaCl_2$, activated μ-calpain (0.5 U) cleaved Hsp70.1 protein involved into the C-terminal fragments of approximately 30~32 kDa (Figure 4-A). Calpain-mediated Hsp70.1 cleavage was negligible using the control (non-oxidized) CA1 tissue, but remarkably increased after incubation in the 1.0 mM H_2O_2 or 500 μM HNE. Such increment of cleavage occurred especially after the oxidative stress-induced carbonylation similarly in each tissue studied, but the naive Hsp70.1 in each tissue showed a very little cleavage. The same was observed using other brain tissues such as thalamus, putamen, globus pallidus and medulla oblongata (data not shown here). Despite the drastic cleavage of carbonylated Hsp70.1, however, this cleavage

was blocked in the presence of ALLN (Figure 4-B). Blockage of Hsp70.1 cleavage occurred dose-dependently with the concentration of ALLN, and cleavage of carbonylated Hsp70.1 was completely blocked in the presence of 100 μM ALLN. It is suggested from these data that Hsp70.1 is an *in-vivo* substrate for activated μ-calpain, and carbonylated Hsp70.1 is extremely vulnerable to the calpain cleavage.

Immunolocalization of Hsp70.1, HNE and activated μ-calpain: In the non-ischemic neurons, immunoreactivities of Hsp70.1, HNE and activated μ-calpain were all negligible or very weak. From day 3 until day 5 after ischemia/reperfusion, however, each immunoreactivity became increasingly intense, compared to the control. On day 5, immunostaining showed a coarsely granular pattern in the perikarya (Figure 2-C). Hsp70.1, HNE or activated μ-calpain were all colocalized with lamp-2, which indicated translocation of each molecule to the lysosomal membrane (lamp-2 data not shown here). Immunoreactivities of HNE and activated μ-calpain became similarly enhanced after ischemia/reperfusion, compared to the control. Hsp70.1 was colocalized with HNE or activated μ-calpain as a fine granular pattern on day 3. Double-positive granular structures became gradually enlarged on day 5, compared to the control (Figure 2-C). These data suggested that Hsp70.1 can spatially become a target of the HNE-mediated carbonylation at the lysosomal membrane, and carbonylated Hsp70.1 can become a substrate of activated μ-calpain at the lysosomal membranes of the postischemic CA1 neurons.

Molecular species and immunoreactivity of BMP: BMP contained a larger amount of C18:1-C18:1 and C22:6-C22:6 (C18:1, oleic acid, C22:6, docosahexaenoic acid). Furthermore, BMP contained a small amount of fatty acids such as C16:1-C18:1, C16:0-C18:1, C18:1-C18:2, C16:0-C22:6, C18:1-C20:4, C20:4-C20:4, C18:1-C22:6, and C20:4-C22:6. Most of the fatty acids studied showed no significant change, but C18:1-C18:1 showed a significant decrease on day 1, compared to the non-ischemic controls ($P<0.05$), and recovered to

Figure 4: *In-vitro* cleavage of Hsp70.1 being involved in various brain tissues from the non-ischemic monkey by activated μ-calpain.
A: 0.5 U μ-calpain being activated by 1.0 mM $CaCl_2$ failed to cleave Hsp70.1 in the CA1 tissue sufficiently (dot red circle), but after carbonylation by 1.0 mM H_2O_2, the cleavage of Hsp70.1 occurred more drastically not only in CA1 (red circle) but also in other brain regions. HNE showed similar facilitation effects upon calpain-mediated Hsp70.1 cleavage (data not shown here). CA1: cornu *Ammonis* 1, DG: dentate gyrus.
B: Blockage of calpain-mediated cleavage of carbonylated-Hsp70.1 in CA1 by a specific calpain inhibitor ALLN. ALLN dose-dependently blocked cleavage of Hsp70.1 being carbonylated by 500 μM HNE. Similarly, ALLN dose-dependently blocked cleavage of Hsp70.1 being involved in other brain regions.

the control level on days 3 and 7. In addition, C22:6-C22:6 showed a significant decrease on days 1 (P<01) and day 3 (P<0.05), compared to the non-ischemic controls, and recovered to the control level on day 7 (Figure 5-A). The average level ± standard deviation (pmol/mg protein) was 65.04 ± 20.88 (control), 37.29 ± 7.86 (day 1), 56.48 ± 21.15 (day 3) and 70.40 ± 3.04 (day 7) for C18:1-C18:1, while it was 105.84 ± 17.38 (control), 54.50 ± 10.86 (day 1), 74.78 ± 16.18 (day 3) and 103.43 ± 20.70 (day 7) for C22:6-C22:6.

In the normal CA1 neurons, BMP immunoreactivity showed a granular pattern. However, on days 3 (Figure 5-B), 5 and 7 after ischemia/reperfusion, immunopositive BMP granules showed a significant decrease, compared to the non-ischemic control. In the normal CA1 neurons, ceramide immunoreactivity showed a coarsely-granular pattern or the whole perinuclear staining. However, on days 3 and 5 after ischemia/reperfusion, fluorescent intensities of the ceramaide also showed a significant decrease, compared to the control (data not shown here). The gradual increase of immunoreactivities of Hsp70.1, HNE and activated μ-calpain (Figure 2-C) occurred simultaneously with the gradual decrease of immunoreactivities of BMP after ischemia/reperfusion (Figure 5-B).

Discussion

Hsp70.1-mediated lysosomal stabilization/destabilization

The major function of lysosomes is to maintain cellular homeostasis by recycling aged/damaged organelles and long-lived proteins. Autophagy is the main process for recycling of organelles and parts of the cytoplasm, and their removal provides nutrient supplies to survive. Intraluminal membranes of lysosomes are characterized by abundant lysosomespecific anionic phospholipid, BMP [27,28]. In this study, BMP immunoreactivity of the CA1 neurons showed a decrease on days 3, 5 and 7 after ischemia (Figure 5-B). One characterisic of BMP is an incorporation of many kinds of polyunsaturated fatty acid-pairs (Figure 5-A) including C22:6 (docosahexaenoic acid) and C18:1 (oleic acids), which may confer specific biophysical and functional properties. It is likely that BMP molecules containing abundant C22:6 and C18:1 will favour increased membrane fusion with Hsp70.1 and/or lysosomal internal membranes owing to their flexibility. Accordingly, decrease of C22:6 and 18:1 would lead to impaired fusion between limiting and internal membranes in lysosomes, which may cause lysosomal membrane destabilization. The postischemic CA1 developed neuronal death on day 5 (Figure 2-A), instead, marked proliferation of microglia and reactive astrocytes that phagocytized neuronal cell debris was seen on day 7 [2,3]. It is conceivable that decrease of C18:1 and C22:6 on days 1 and 3 (i.e., BMP degradation) is related to neuronal death, whereas recover of both on day 7 (BMP re-synthesis) (Figure 5-A) is related to the reactive cell proliferation.

Hsp70.1-BMP binding is indispensable for stabilizing lysosomal membrane and promoting cell survival [29]. Large amounts of BMP in the lysosomal internal membranes distinguish it from the limiting membrane. BMP is required for sphingolipid degradation at the internal membranes in the acidic compartments. BMP binds acid sphingomyelinase (ASM) and stimulates its ability to hydrolyse sphingomyelin to produce ceramide [30-32]. Ceramide at the lysosomal membrane can stabilize lipid phases, i.e., microdomains, more efficiently than cholesterol [33,34]. Ceramide protects the lysosomal membrane from rupturing [29,35,36], because the increased concentration of lysosomal ceramide possibly facilitates fusion of lysosomes with other intracellular vesicles and membranes [37]. Both
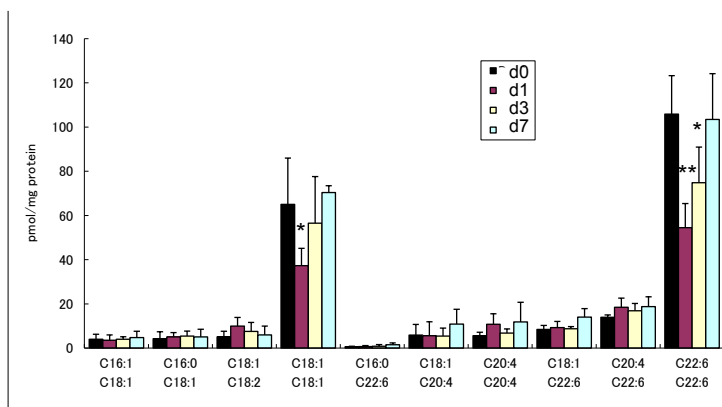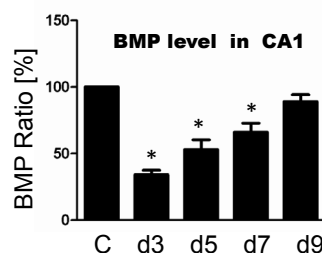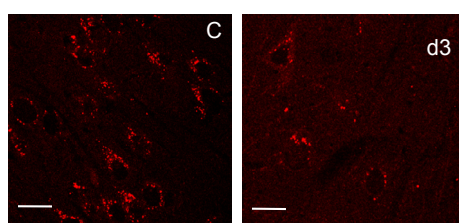
Figure 5: Dynamic changes of molecular species of lysosomal BMP and its immunoreactivity.
A: The contents of each molecular species of BMP were determined by LC-MS using the monkey CA1 tissues (n=4 for each group). C18:1-C18:1 shows a significant (*p<0.05) decrease on day 1 (d1) after ischemia/reperfusion, and C22:6-C22:6 shows significant decreases on day 1 (d1: **p<0.01) and day 3 (d3: *p<0.05). Both show a recover to the control levels (d0) on day 7 (d7).
B: BMP fluorescent intensity of CA1 neurons on days 3 (d3), 5 (d5) and 7 (d7) shows a significant (*p<0.05) reduction, compared to the control (C). Scale bar=20 μm.
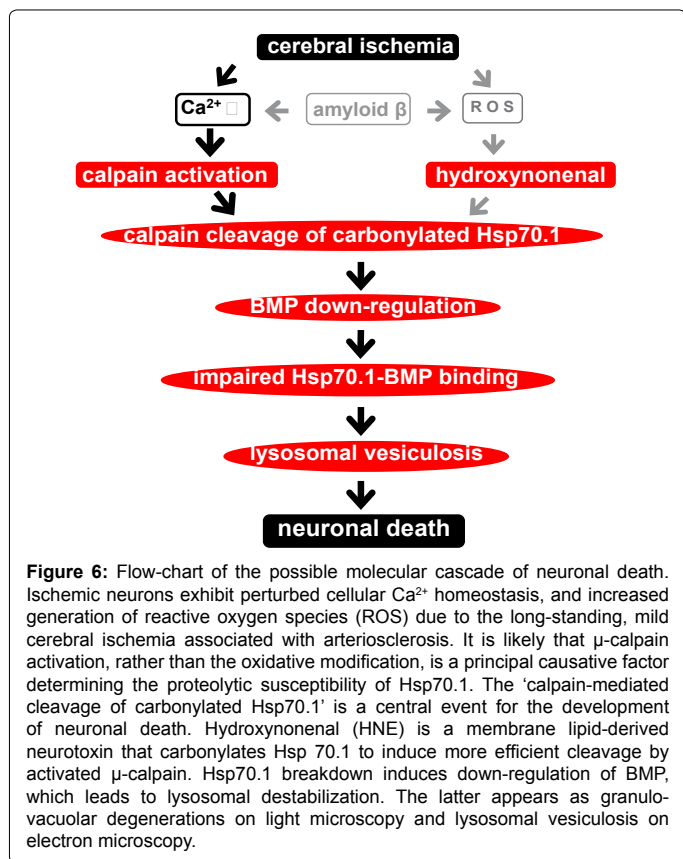
molecular species and immunofluorescent analyses showed down-regulation of BMP on days 1~3 (Figure 5). BMP down-regulation, combined with Hsp70.1 cleavage, presumably provoked impairment of ASM with accumulation of syphingomyelin and deficiency of ceramide at the lysosomal membrane.

Lysosomes are rich in redox-active iron and favor Fenton-type-mediated generation of hydroxyl radicals, which results in enhanced lipid peroxidation of lysosomal membranes and carbonylation of Hsp70.1. As shown in Figure 4, Hsp70.1, especially after its carbonylation, became prone to calpain-mediated cleavage *in-vitro*. The same cleavage was shown to occur using various brain regions such as DG, motor cortex, cerebellar cortex and substantia nigra. Furthermore, in other brain regions studied, calpain cleavage was very little in the absence of oxidative modification, but increased after carbonylation. Regardless of the brain regions, the intensity of the cleaved band was almost equal. Xue et al. [38] demonstrated that artificial carbonylation of myofibrillar proteins by oxygen radicals increased μ-calpain-mediated cleavage of myosin heavy chain andα-actinin, but had no influence on cleavage of actin, and even reduced that of troponin-T. Importantly, only in the presence of calpain activation the cleavage occurred, and the increasing oxidative level caused a stepwise escalation in cleavage, which coincides well with the stepwise carbonyl increase. However, in the absence of calpain activation, even the maximum protein oxidation could not cause a spontaneous breakdown of myofibrillar proteins. Taken together, μ-calpain activation may be a principal factor affecting Hsp70.1 susceptibility (Figures 4 and 6).

Similarity between ischemic and degenerative neuronal death

Dysfunction of Hsp70.1 and/or deficiency of ASM are closely

Figure 6: Flow-chart of the possible molecular cascade of neuronal death. Ischemic neurons exhibit perturbed cellular Ca^{2+} homeostasis, and increased generation of reactive oxygen species (ROS) due to the long-standing, mild cerebral ischemia associated with arteriosclerosis. It is likely that μ-calpain activation, rather than the oxidative modification, is a principal causative factor determining the proteolytic susceptibility of Hsp70.1. The 'calpain-mediated cleavage of carbonylated Hsp70.1' is a central event for the development of neuronal death. Hydroxynonenal (HNE) is a membrane lipid-derived neurotoxin that carbonylates Hsp 70.1 to induce more efficient cleavage by activated μ-calpain. Hsp70.1 breakdown induces down-regulation of BMP, which leads to lysosomal destabilization. The latter appears as granulo-vacuolar degenerations on light microscopy and lysosomal vesiculosis on electron microscopy.

associated with the lysosomal rupture [15,16]. Both can occur in cerebral ischemia, whereas only ASM deficiency occurs in Niemann-Pick type A disease. The latter is a recessively inherited disorder due to mutations in the sphingomyelin phosphodiesterase 1 gene, and the reduced activity of ASM causes sphingomyelin accumulation [39,40]. The Niemann-Pick patients develop progressive neurodegeneration including cerebral and cerebellar atrophy, relevant Purkinje cell and myelin deficiency. Purkinje cells containing abundant membrane lipids because of its giant size, might reveal sufficient lysosomal lipidosis prior to its disruption. It is likely that disorders of both Hsp70.1 and ASM cause CA1 neuronal death within a week, whereas a few years may be necessary for Purkinje cells to degenerate only by ASM deficiency, and in the absence of Hsp70.1 dysfunction [15].

In AD, not only chronic hypoxia but also amyloid β depositions will sustain calpain activation [41-43]. Furthermore, the free HNE elevations have been detected in the cerebrospinal fluid of AD patients [44]. Immunohistochemical analyses of the postmortem brain tissue from AD or Parkinson patients revealed increased protein modification by HNE [45,46]. AD is a disorder associated with autophagic- lysosomal dysfunction; 'calpain-mediated cleavage of Hsp70.1' appears to be an instigator of degenerative neuronal death associated with AD [16].

Neuronal survival requires continuous lysosomal turnover of long-lived cellular constituent proteins, lipids and organelles that were delivered by autophagy. After internalization, for example, cell surface proteins and lipids are returned to the plasma membrane via recycling endosomes. Declining autophagic-lysosomal degradative efficiency of cellular debris, causes accumulation of undigested lipid and protein. This eventually leads to autophagic vacuole accumulation and/or lysosomal destabilization as a basis for the degeneration in aged neurons. In this study, a continuum of abnormalities of the lysosomal system was identified in neurons of the ischemic monkey and Alzheimer neurons, including a concomitant and progressive disruption of autophagy, and the massive build-up of incompletely digested cell proteins and membrane lipids. Calpain-mediated cleavage of carbonylated Hsp70.1 may contribute to establishing a relationship between pathological hallmarks of ischemic and degenerative neuronal death (Figure 6). The calpain-cathepsin cascade [2,3] would contribute to neurodegeneration with accumulations of autophagic vacuoles being observed as granulo-vacuolar degeneration by light microscopy while as lysosomal vesiculosis by electron microscopy. Lysosomes seem to be well protected against external damage, with Hsp70.1 being one of the important guardians against cellular stresses [29,47]. Because most AD cases are sporadic, the most important risk factor should be age-related lysosomal destabilizations.

Summary

In the monkey brains after ischemia/reperfusion, both calpain activation during ischemia and Hsp70.1 carbonylation during reperfusion, were demonstrated to cause programmed neuronal necrosis. The latter may occur for days by acute cerebral ischemia whereas for years by long-standing cerebral ischemia. The pathogenic synergism between calpain activation and Hsp70.1 carbonylation works in concert to destabilize lysosomal membranes via BMP down-regulation (Figure 6). Since Hsp70.1 carbonylation occurs in any brain regions but neuronal death predominantly occurs in the CA1, the extent of calpain activation would be a key factor determining the cell death fate. The present study focusing lysosomal destabilization due

to the 'calpain-mediated cleavage of carbonylated Hsp70.1' suggests a conceptual framework to further understand the mechanism of ischemic neuronal death and its potential relevance to Alzheimer neuronal death. The authors apeculate that 'lysosomal vesiculosis' is a common ultrastructural feature downstream to all pathological conditions involving the brain, regardless of the cause.

Acknowledgements

Conflict of Interest

References

1. De Duve C, Pressman BC, Gianetto r, Wattiaux R, Appelmans F (1955) Tissue fractionation studies. 6. Intracellular distribution patterns of enzymes in rat-liver tissue. Biochem J 60: 604-617.

2. Yamashima T, Kohda Y, Tsuchiya K, Ueno T, Yamashita J, et al. (1998) Inhibition of ischaemic hippocampal neuronal death in primates with cathepsin B inhibitor CA-074: a novel strategy for neuroprotection based on 'calpain-cathepsin hypothesis'. Eur J Neurosci 10: 1723-1733.

3. Yamashima T, Saido TC, Takita M, Miyazawa A, Yamano J, et al. (1996) Transient brain ischaemia provokes Ca2+, PIP2 and calpain responses prior to delayed neuronal death in monkeys. Eur J Neurosci 8: 1932-1944.

4. West MJ, Coleman PD, Flood DG, Troncoso JC (1994) Differences in the pattern of hippocampal neuronal loss in normal ageing and Alzheimer's disease. Lancet 344: 769-772.

5. Butterfield DA, Drake J, Pocernich C, Castegna A (2001) Evidence of oxidative damage in Alzheimer's disease brain: central role for amyloid beta-peptide. Trends Mol Med 7: 548-554.

6. Butterfield DA, Lauderback CM (2002) Lipid peroxidation and protein oxidation in Alzheimer's disease brain: potential causes and consequences involving amyloid ß-peptide-associated free radical oxidative stress. Free Radic Biol Med 32: 1050-1060.

7. Kragh CL, Ubhi K, Wyss-Coray T, Masliah E (2012) Autophagy in dementias. Brain Pathol 22: 99-109.

8. Halliwell B (2006) Oxidative stress and neurodegeneration: where are we now? J Neurochem 97: 1634-1658.

9. Dalle-Donne I, Scaloni A, Giustarini D, Cavarra E, Tell G, et al. (2005) Proteins as biomarkers of oxidative/nitrosative stress in diseases: the contribution of redox proteomics. Mass Spectrom Rev 24: 55-99.

10. Esterbauer H, Schaur RJ, Zollner H (1991) Chemistry and biochemistry of 4-hydroxynonenal, malonaldehyde and related aldehydes. Free Radic Biol Med 11: 81-128.

11. Schneider C, Tallman KA, Porter NA, Brash AR (2001) Two distinct pathways of formation of 4-hydroxynonenal. Mechanisms of nonenzymatic transformation of the 9- and 13-hydroperoxides of linoleic acid to 4-hydroxyalkenals. J Biol Chem 276: 20831-20838.

12. Uchida K (2003) 4-Hydroxy-2-nonenal: a product and mediator of oxidative stress. Prog Lipid Res 42: 318-343.

13. Oikawa S, Yamada T, Minohata T, Kobayashi H, Furukawa A, et al. (2009) Proteomic identification of carbonylated proteins in the monkey hippocampus after ischemia-reperfusion. Free Radic Biol Med 46: 1472-1477.

14. Yamashima T, Oikawa S (2009) The role of lysosomal rupture in neuronal death. Prog Neurobiol 89: 343-358.

15. Yamashima T (2012) Hsp70.1 and related lysosomal factors for necrotic neuronal death. J Neurochem 120: 477-494.

16. Yamashima T (2013) Reconsider Alzheimer's disease by the 'calpain-cathepsin hypothesis'--a perspective review. Prog Neurobiol 105: 1-23.

17. Kalaria RN, Ballard C (1999) Overlap between pathology of Alzheimer disease and vascular dementia. Alzheimer Dis Assoc Disord 13 Suppl 3: S115-123.

18. Kalaria RN (2000) The role of cerebral ischemia in Alzheimer's disease. Neurobiol Aging 21: 321-330.

19. Kalaria RN (2002) Small vessel disease and Alzheimer's dementia: pathological considerations. Cerebrovasc Dis 13 Suppl 2: 48-52.

20. Pluta R, Ułamek M, Jabłoński M (2010) Consideration of the ischaemic basis and treatment of Alzheimer's disease. Folia Neuropathol 48: 11-26.

21. Vermeer SE, Prins ND, den Heijer T, Hofman A, Koudstaal PJ, et al. (2003) Silent brain infarcts and the risk of dementia and cognitive decline. N Engl J Med 348: 1215-1222.

22. Kobayashi T, Stang E, Fang KS, de Moerloose P, Parton RG, et al. (1998) A lipid associated with the antiphospholipid syndrome regulates endosome structure and function. Nature 392: 193-197.

23. Kikuchi H, Imajoh-Ohmi S (1995) Activation and possible involvement of calpain, a calcium-activated cysteine protease, in down-regulation of apoptosis of human monoblast U937 cells. Cell Death Differ 2: 195-199.

24. Saido TC, Nagao S, Shiramine M, Tsukaguchi M, Sorimachi H, et al. (1992) Autolytic transition of mu-calpain upon activation as resolved by antibodies distinguishing between the pre- and post-autolysis forms. J Biochem 111: 81-86.

25. Bligh EG, Dyer WJ (1959) A rapid method of total lipid extraction and purification. Can J Biochem Physiol 37: 911-917.

26. Funk KE, Mrak RE, Kuret J (2011) Granulovacuolar degeneration (GVD) bodies of Alzheimer's disease (AD) resemble late-stage autophagic organelles. Neuropathol Appl Neurobiol 37: 295-306.

27. Schulze H, Kolter T, Sandhoff K (2009) Principles of lysosomal membrane degradation: Cellular topology and biochemistry of lysosomal lipid degradation. Biochim Biophys Acta 1793: 674-683.

28. Kolter T, Sandhoff K (2010) Lysosomal degradation of membrane lipids. FEBS Lett 584: 1700-1712.

29. Kirkegaard T1, Roth AG, Petersen NH, Mahalka AK, Olsen OD, et al. (2010) Hsp70 stabilizes lysosomes and reverts Niemann-Pick disease-associated lysosomal pathology. Nature 463: 549-553.

30. Linke T, Wilkening G, Lansmann S, Moczall H, Bartelsen O, et al. (2001) Stimulation of acid sphingomyelinase activity by lysosomal lipids and sphingolipid activator proteins. Biol Chem 382: 283-290.

31. Linke T, Wilkening G, Sadeghlar F, Mozcall H, Bernardo K, et al. (2001) Interfacial regulation of acid ceramidase activity. Stimulation of ceramide degradation by lysosomal lipids and sphingolipid activator proteins. J Biol Chem 276: 5760-5768.

32. Kolter T, Sandhoff K (2005) Principles of lysosomal membrane digestion: stimulation of sphingolipid degradation by sphingolipid activator proteins and anionic lysosomal lipids. Annu Rev Cell Dev Biol 21: 81-103.

33. Massey JB (2001) Interaction of ceramides with phosphatidylcholine, sphingomyelin and sphingomyelin/cholesterol bilayers. Biochim Biophys Acta 1510: 167-184.

34. Xu X, Bittman R, Duportail G, Heissler D, Vilcheze C, et al. (2001) Effect of the structure of natural sterols and sphingolipids on the formation of ordered sphingolipid/sterol domains (rafts). Comparison of cholesterol to plant, fungal, and disease-associated sterols and comparison of sphingomyelin, cerebrosides, and ceramide. J Biol Chem 276: 33540-33546.

35. Petersen NH, Kirkegaard T (2010) HSP70 and lysosomal storage disorders: novel therapeutic opportunities. Biochem Soc Trans 38: 1479-1483.

36. Petersen NH, Kirkegaard T, Olsen OD, Jäättelä M (2010) Connecting Hsp70, sphingolipid metabolism and lysosomal stability. Cell Cycle 9: 2305-2309.

37. Heinrich M, Wickel M, Winoto-Morbach S, Schneider-Brachert W, Weber T, et al. (2000) Ceramide as an activator lipid of cathepsin D. Adv Exp Med Biol 477: 305-315.

38. Xue M, Huang F, Huang M, Zhou G (2012) Influence of oxidation on myofibrillar proteins degradation from bovine via μ-calpain. Food Chemistry 134: 106-112.

39. Brady RO, Kanfer JN, Mock MB, Fredrickson DS (1966) The metabolism of sphingomyelin. II. Evidence of an enzymatic deficiency in Niemann-Pick diseae. Proc Natl Acad Sci U S A 55: 366-369.

40. Schuchman EH (2007) The pathogenesis and treatment of acid

sphingomyelinase-deficient Niemann-Pick disease. J Inherit Metab Dis 30: 654-663.

41. Saito K, Elce JS, Hamos JE, Nixon RA (1993) Widespread activation of calcium-activated neutral proteinase (calpain) in the brain in Alzheimer disease: a potential molecular basis for neuronal degeneration. Proc Natl Acad Sci U S A 90: 2628-2632.

42. Taniguchi S, Fujita Y, Hayashi S, Kakita A, Takahashi H, et al. (2001) Calpain-mediated degradation of p35 to p25 in postmortem human and rat brains. FEBS Lett 489: 46-50.

43. Higuchi M, Iwata N, Matsuba Y, Takano J, Suemoto T, et al. (2012) Mechanistic involvement of the calpain-calpastatin system in Alzheimer neuropathology. FASEB J 26: 1204-1217.

44. Lovell MA, Ehmann WD, Mattson MP, Markesbery WR (1997) Elevated 4-hydroxynonenal in ventricular fluid in Alzheimer's disease. Neurobiol Aging 18: 457-461.

45. Yoritaka A, Hattori N, Uchida K, Tanaka M, Stadtman ER, et al. (1996) Immunohistochemical detection of 4-hydroxynonenal protein adducts in Parkinson disease. Proc Natl Acad Sci U S A 93: 2696-2701.

46. Sayre LM, Zelasko DA, Harris PL, Perry G, Salomon RG, et al. (1997) 4-Hydroxynonenal-derived advanced lipid peroxidation end products are increased in Alzheimer's disease. J Neurochem 68: 2092-2097.

47. Nylandsted J, Gyrd-Hansen M, Danielewicz A, Fehrenbacher N, Lademann U, et al. (2004) Heat shock protein 70 promotes cell survival by inhibiting lysosomal membrane permeabilization. J Exp Med 200: 425-435.